SigmaJournal of Engineeringand Natural Sciences, Vol. 42, No. 6, pp. XX-XX, December, 2024
Yildiz Technical University Press, Istanbul, Turkey

The effect of marble waste in the production of low-temperature porous material from Alkali-activated fly ash

Hakan CENGIZLER[1], Muhterem KOÇ[2*]

ABSTRACT

The production of low-cost open-pore ceramic materials from fly ash (FA) and marble waste (MW) was investigated.The effect of MW (5-40 wt.%) onthe open porosity was determined. To reduce the sintering temperature and improve the properties of porous materials, the mixtures were activated with an alkali solution. Samples pressed from FA and FA+MW mixtures were sintered at low temperature (900 °C), but sufficient strength could not be obtained. However, when these mixtureswere subjected to alkali activation, pressed and sintered at 900 °C, sufficient strength and porosity values were reached. The open porosity of the MW neat specimen was 12.70%, but it increased up to 39.91% at 40 wt.% MW, which was the highest ratio used in the literature. The main phase structure was nepheline at 0-20 wt.% MW, but gehlenite became the dominant phase at 40 wt. % MW. The compressive and flexural strength values of 40 wt.% MW added specimen was determined to be 12 and 5.35 MPa, respectively.The open-pore ceramic of high MW ratio, produced by this new alternative route, has the potential for use in water purification membranes for macro filtration purposes.

Keywords: *Fly ash, Marble waste, Alkali activation, Sintering, Open-pore*

INTRODUCTION

Porous ceramics have beneficial properties such ashigh mechanical, thermal and chemical stability, long lifetime, high permeability, ease of cleaningwith many other advantages[1–3].The microstructure of porous ceramics can be tailored and have a slight polluting effect on the environment[4] along with properties such as less susceptibility to microbial attacks and biological degradations[5]. All these superior properties, in contrast to those of polymeric porous materials, have found applications in engineering practices such as membranes in filtration processes[4,5], catalysis applications[6], thermal isolation coatings[7], and porous bricks[8].

Because of the high costs of precursor materials used to manufacture open-pore ceramics[9,10],natural clays such as kaolin and ball clay, feldspar and quartz sand as well as industrial waste substances were used as mainraw materials. In this regard, research was especially directed towards producing new generation inorganic porous products at a low price manufactured from many low-cost waste materials causing environmental pollution.FA[3,4], steel slag [10], glass waste[6], screen and monitor glass waste[11], sewage sludge[12], paper sludge[13], biological waste of water purification[14], coal extraction waste[15], sandblasting waste[16], wasted diatomaceous earths[11,16], coffee waste[17], and red mud[18] were a few of them. FA is a waste generated in large amounts during coal combustion in thermal power plants. Any attempt to recycle or re-utilize FA is crucial for the environment. FA, with the addition of pore-forming materials, were sintered and porous ceramic structures were obtained[3,10]. Additionally, it was found that geopolymerization of FA before sintering had a positive effect on the material properties[19,20]. Besides, geopolymerization made it possible to produce materials at lower temperatures[21].Previous studies showed that the physical and mechanical properties of FA-

[1]*Manisa Celal Bayar University, Turgutlu Vocational School, The Department of Materials and Materials Processing Technologies, 45410 Turgutlu, Turkey*

[2]*Kütahya Dumlupınar University, Department of Industrial Design, Kütahya, 43100, Turkey*

[*] *E-mail: muhterem.koc@dpu.edu.tr*

Orcidid:https://orcid.org/0000-0001-5982-7692 Hakan Cengizler, 0000-0003-3661-4410 Muhterem Koç

This paper was recommended for publication in revised form by Regional Editor AhmetSelimDalkilic
[1]Manisa Celal Bayar University, Turgutlu Vocational School, The Department of Materials and Materials Processing Technologies, 45410 Turgutlu, Turkey
[2]Kütahya Dumlupınar University, Department of Industrial Design, Kütahya, 43100, Turkey
**E-mail address: muhterem.koc@dpu.edu.tr*
Orcid id:[1]https://orcid.org/0000-0001-5982-7692 Hakan Cengizler, 0000-0003-3661-4410 Muhterem Koç
Manuscript Received 09 January 2023, Revised 16 February 2023, Accepted 04 April 2023

based geopolymers exposed to elevated temperatures improved[20]. It was stated that FA-based geopolymers had large numbers of small pores, which facilitated the escape of moisture when exposed to elevated temperatures, thus causing minimal damage to the geopolymer[19].Sintering resulted in densification and development of new phases in the structure[19] and improved the properties of geopolymers[19,20]. Furthermore, densification and formation of new phases were reported at and above 900°C[19,20,22]. In conclusion, exposure to high temperature resulted in sintering processes, structural rearrangement and new crystalline phases contributing to strength[23].

Previous work also studied the performance of porous geopolymers made with FA after exposure to high temperatures. Abdullah et al.[24]prepared geopolymer paste samples by alkali activation of FA with a mixture of sodium hydroxide and sodium silicate solution. They cured the geopolymer paste samples at 60 °C for 24 h and sintered them at the range of 600-1000°C. In a very recent study, Sawan et al.[25] investigated the in-situ formation of geopolymer foams from metakaolin. They used an alkali activator solution of sodium silicate and sodium hydroxide to prepare the initial geopolymer pastes. Afterwards,they sintered the samples at 800, 1000 and 1200°C. In the studies mentioned above[24,25], they produced porous geopolymer materials first and then subjected them to the sintering process. Thus, they investigated the effect of sintering on geopolymer materials. Geopolymer technology enables the production of high-performance ceramics at a lower temperature compared to those produced by conventional sintering[21].However, geopolymer materials produced from FA do not have enough open porosity before and after sintering. Therefore, additives are needed to increase porosity.Carbonates decompose well below 1000 °C releasing CO_2 gas. Therefore, calcite, dolomite and soda ash containing carbonates in their structurewere studied extensively as pore making agents.The recent work on porous ceramic productionwas also focused onexploring novel pore forming additives such as activated carbon, natural phosphates, wood sawdust, and raw materials containingcarbonates, etc.[9].In this regard, the use of MW as a carbonate source should be investigated instead of the pore making carbonate sources mentioned above. Thus, the damage to the environment will be mitigated and the production cost of porous ceramics will be reduced.

The present studyinvestigatedthe utilization of MW as a pore-making agentin the production of open-pore ceramic from FA.The experimental compositions were activated with an alkali solution of Na_2SiO_3 and NaOH, which also have a fluxingeffect, to reduce sintering temperature.The effect of adding MW in different ratios (5-40 wt.%) into FA on open porosity, new phase formation, mechanical and physical properties wasinvestigated.The utilization of these industrial wastes as main raw materials to manufacture porous ceramics would be beneficial with effective solid waste management and reduced production costs.

MATERIALS AND METHODS

Materials

The Tunçbilek FA was collected from Tunçbilek thermal power plant (Kütahya, Turkey). A marble processing plant (Karaburun, Turkey) provided MW. Chemical grade NaOH and Na_2SiO_3 were purchased from Merck Chemicals GmbH.

Processing and characterization

Five specimens of different geopolymer compositions were prepared (Table 1). The first one consisted of 100 wt. % Tunçbilek FA and was coded as MW0. The other five specimens were prepared by gradually increasing MW ratios of 5, 10, 20, and 40 wt. % coded as MW5, MW10, MW20, and MW40, respectively. The numbers following the denotation show wt. % of MW.

Firstly, the Tunçbilek FA and the MW, totally 100 grams, were homogeneously dry mixed according to the predetermined ratios (Table 1). Previously prepared 12M alkali solution of NaOH and Na_2SiO_3 was added (Table 1) and mixed for 5 minutes using a laboratory mixer. Homogeneously mixed compositions were shaped into specimens of 10x10x55 mm dimensions under 50 MPa pressure using a hydraulic press. Subsequently, they were dried at 105°C for 24 hours in a laboratory drier. Curing and drying processes were combined and carried out simultaneously in a single stage of 24 hours, which was cost-effective and time-saving. After completing the drying stage, the alkali-activated specimens were sintered at 900 ℃ for 30 minutes with a ramping rate of 5°C/min. Finally, the sintered specimens were characterized.

The chemical analyses of the Tunçbilek FA and the MW were carried out by X-ray fluorescence (XRF) (PanalyticalAxios). Phase identification was conducted by X-ray diffraction (XRD) on raw materials and porous

ceramic specimens using a RigakuMiniflex powder diffractometer with Cu Kα radiation (λ=1.5418 Å). The measuring rate was 2°/min at 40 kW and 30 mA in the 15–70° 2θ range. Crystallographic databases used for the phase identifications were Inorganic Crystal Structure Database (ICSD) and International Centre for Diffraction Data (ICDD) PDF-2. The thermal behaviour of the Tunçbilek FA and the MW was investigated using a fully computer-controlled DTA/TG (Netzsch STA 449F3). The measurement, for the MW, was conducted between room temperature and 1100°C. It was conducted, for the Tunçbilek FA, between room temperature and 1300°C. The heating rate was 10°C/min in the air during both measurements. The particle size distribution of the Tunçbilek FA and the MW was determined using a laser size analyzer (Malvern). Scanning electron microscopy (SEM) was conducted on a Nova NanoSEM650 scanning electron microscope to investigate the microstructure of the waste materials (FA and MW) and the sintered geopolymer specimens on the fractured surfaces. Polished cross-sections were produced by mounting sample fragments in low viscosity epoxy resin and polishing to a 1 μm finish. Samples were coated with a thin layer of Au-Pt before SEM imaging.

Bulk density, apparent porosity (open porosity), water absorption[26], and compressive strength[27] were determined according to the related standards. The compressive strength tests were carried out using a hydraulic press (SACMI 470, PIL type) with a speed of 0.5 mm/min. Five specimens were tested for each composition and the average values of the compressive strength were calculated. The flexural strength (three-point bending strength) was measured using Shimatsu 250 kN Model equipment. Again, the average values of the flexural strength were calculated from the results of five specimens tested for each composition. The linear shrinkage values of the sintered geopolymer specimens were measured by subtracting the fired length from the original green length[28].

The bulk density was measured according to Archimedes' principle. The powder density was calculated by a pycnometer. The open porosity (P) was calculated from the dry, soaked (in water) and suspended (in water) weights of a specimen using equation 1:

$$\%P: \frac{(Soaked\ Weight - Dry\ Weight)}{(Soaked\ Weight - Suspended\ Weight)} \quad (1)$$

Water absorption value represents the open porosity. It was calculated by the difference in specimen weight under over-dried and fully saturated (in water) conditions[26].

Table 1. Geopolymer compositions and codes.

Sample code	MW0	MW5	MW10	MW20	MW40
FA (g)	100	95	90	80	60
MW (g)	-	5	10	20	40
NaOH (g)	20	20	20	20	20
Na_2SiO_3(g)	20	20	20	20	20

RESULTS AND DISCUSSION

Characterization of the raw materials

In Table 2, the chemical composition of the Tunçbilek FA used as the main material and the MW, as a pore-forming agent, was given. The sum of SiO_2, Al_2O_3 and Fe_2O_3 was 87.44 wt. % showing that the Tunçbilek FA was F class[29]. The Tunçbilek FA also contained MgO (4.48 wt. %) and CaO (1.64 wt. %) along with minor quantities of K_2O, Na_2O, and SO_3. LOI value of the Tunçbilek FA was 4.08 wt. %. The MW contained 61.65 wt. % CaO and a low amount of SiO_2 (2.20 wt. %), MgO (0.69 wt. %), Al_2O_3 (0.19 wt. %), and Fe_2O_3 (0.06 wt. %). The LOI value of the MW was 35.08 wt. %, which correlates well with the reported values[30,31].

When looked at the phase analysis, quartz, haematite and mullite were detected to be the main crystalline phases in the Tunçbilek FA (Figure 1). The origin of quartz (primary quartz) in the Tunçbilek FA was the source coal and the secondary quartz formed during combustion[32]. The mullite was the product of the solid-state reaction of decomposed clays[32] and/or occurred through the crystallization of the aluminosilicate melt[33]. The existence of haematite, which generally exists in bituminous F class FA, was because of the

thermal decomposition of clay minerals during combustion[34]. Calcite was the only dominant crystalline phase in the MW with a low amount of quartz phase (Figure 1)[35]. The fact that the MW contained a high amount of CaO (61.65 wt. %) (Table 2) enabled it to be a suitable material in its use as a pore former. It was also used as a cheap pore-forming agent because it was a waste material[31,32,35].

Table 2. Chemical analyses of Tunçbilek FA and MW.

Chemical composition (%)	FA (%)	MW (%)
SiO_2	58.26	2.20
Al_2O_3	17.73	0.19
Fe_2O_3	11.45	0.06
CaO	1.64	61.65
MgO	4.48	0.69
K_2O	0.66	-
Na_2O	0.35	-
SO_3	0.26	0.05
LOI*	4.08	35.08

*: Loss of ignition

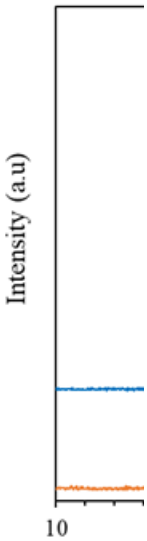

Figure 1. XRD spectrum of Tunçbilek FA (a) and MW (b). (C: calcite, Q: Quartz, M: Mullite, H: Hematite)

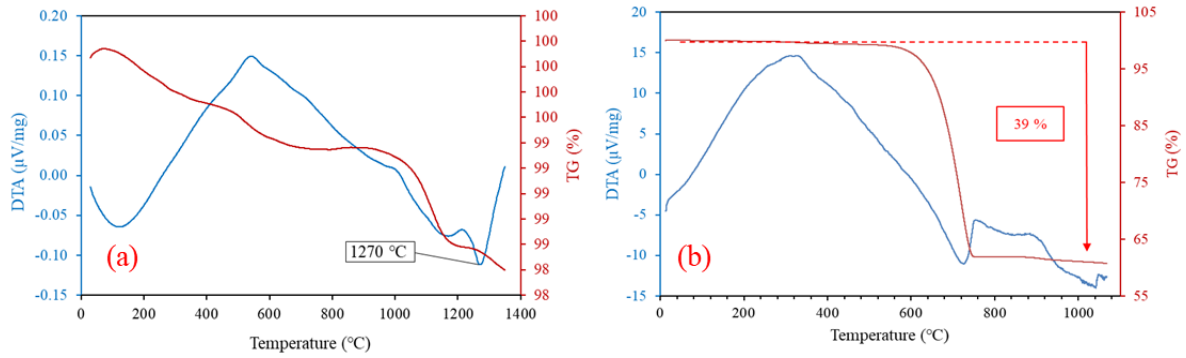

Figure 2. DTA/TG analysis of Tunçbilek FA (a) MW (b).

The thermal behaviourof the Tunçbilek FA was studied by DTA/TG analyses (Figure 2a). First, an endothermic peak on theDTA curve at approximately 160°C corresponded to the evaporation of moisture, that is, dehydration of adsorbed water mechanically bonded in the form of H_2O molecules on the surface of the ash particles[36,37]. In the interval between 100 and 450°C, the removal of hydrated water was completed[38]. Subsequently, an exothermic event at 678°C was associated with the combustion of unburned coal[39]. At higher

temperatures between 800 and 1200°C, the decomposition of impurities from coal, carbonates, or sulphatestook place [36,39]. The TG curve accordingly showed a continuous decrease in weight. The melting temperature of the Tunçbilek FA was 1220°C (Figure 2a).

In the DTA analysis of the MW (Figure 2b), a gradual mass loss of approximately 1.5 % was observed up to 575°C, which can be attributed to moisture loss[31,36]. A sharp endothermic reaction occurred between 620 and 760°C with a rapid downward move in the TG curve. This temperature indicated to the decomposition of calcite according to equation 2. Looking at the TG curve, the MW lost about 39% of its initial weight between 620 and 760°C[30,31]. It was considered that the high loss of ignition (LOI) (Figure 2b) (Table 2), would contribute to the formation of a porous structure in this study. Following equation 2[30,31], it was presumed that the calcium carbonate broke down under heat and converted into CaO (solid) and CO_2 (gas), and open-pore structure formed because of the CO_2 gas released.

$$CaCO_{3(s)} \rightarrow CaO_{(s)} + CO_{2(g)} \quad (2)$$

The size distribution of the Tunçbilek FA (D_{10} 6.09 µm, D_{50} 32.5 µm and D_{90} 124 µm) ranged between 0.46 and 310 µm. However, the particle size distribution of the MW was smaller (D_{10} 2.11 µm, D_{50} 9.17 µm and D_{90} 42.14 µm) than that of the Tunçbilek FA in a close range between 0.46-66 µm (Fig. 3). Therefore, it was considered advantageous in that the pore dimensions are in a narrow range. The Tunçbilek FA and the MW were both used as received with no size-reduction.

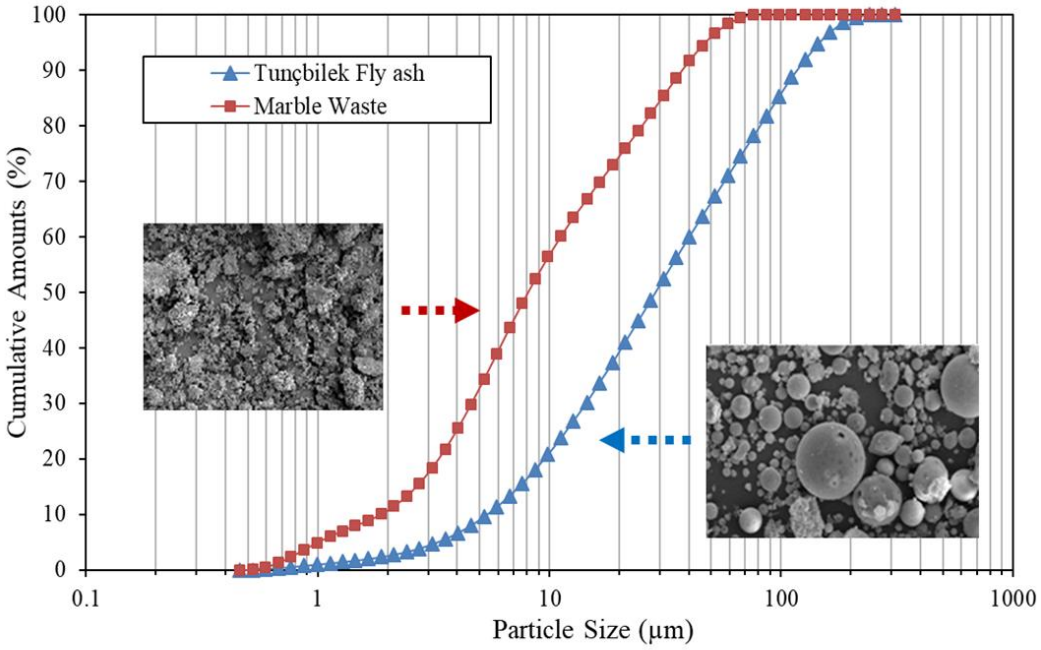

Figure 3. Particle size distribution of Tunçbilek FA and MW.

The Tunçbilek FA mostlyconsisted of spherical particles so-called microspheres with some irregularly shaped angular particles (Figure 3). The MW had a microstructure consisted of irregular but dimensionally similar particles (Figure 3).

In the current experimental work, theproduction of open-pore ceramic from waste materials FA and MW was investigated. The alkali activation method was adopted to reduce the sintering temperature of green specimens to the lowest possible value. As seen from the DTA data in Figure 2b, the decomposition temperature of the MW was between 620 and 760°C[30,31]. The LOI value of the MW was 39 wt. %[30,31]. However, as mentioned earlier, previous studies on sintering of geopolymers showed that densification and formation of new phases in the structure[23], which improved the properties of geopolymers [19,20], occurred at and above 900°C[19,20]. Therefore, in the present work, the alkali-activated specimens composed of the Tunçbilek FA and

the MW were sintered at 900°C, to investigate the effect of sintering on forming an open-pore structure and contribution of new phase development to mechanical properties.

Physico-mechanical properties of sintered porous geopolymers

FTIR analysis is principally based on the absorption of different wavelengths of infrared light and studies the composition and structure of material molecules. Besides, FTIR absorption spectroscopy is an effective tool for characterizing alkali-activated materials because of its well-known sensitivity for materials of short-range structural order[40]. Therefore, FTIR tests were conducted on the raw Tunçbilek FA and alkali-activated compositions to investigate the effect of alkali activation on the FA structural development. The results of the FTIR spectra were depicted in Figs.4a and 4b. In Figure 4a, the effect of alkali activation was determined by examining the raw and alkali-activated FA (MW0) specimen. The central band at around 1022 cm^{-1}, as the main feature of the FTIR spectra of raw FA, exhibited overlapped peaks associated with the asymmetric stretching vibrations of tetrahedral Si-O-Si or Si-O-Al bonds[41]. The intensity of this band is proportional to the reactivity of FA[42]. The peak at 1022 cm^{-1} shifted towards lower wavenumber of 983 cm^{-1} indicating the formation of geopolymer structure due to alkali activation[42,43]. The new peak observed at a lower wavenumber of 983 cm^{-1} on geopolymerization was directly linked with the transformation of Si-O-Si bonds of amorphous silica into Si-O-Al bonds of poly sialate, which meant the substitution of Si by tetrahedral Al and therefore the formation of the geopolymer structure of aluminosilicate network[44]. Another band, which appeared in the geopolymer specimen at around 1440 cm^{-1}, was absent in the Tunçbilek FA. This characteristic band appeared due to the asymmetric vibrations of CO_3^{-2} ions, which pointed to the presence of sodium carbonate because of the carbonation reaction between excess sodium and atmospheric carbon dioxide[42,44]. The band 777 cm^{-1} was connected with the symmetric stretching vibration of Si-O-Si, which was characteristic of quartz. Quartz was also detected in the XRD analysis of the Tunçbilek FA (Figure 1), which supported the FTIR results. The last band observed at around 443 cm^{-1} was assigned to Si-O- and Al-O bending vibrations characteristic for silica glass and silicates[42].

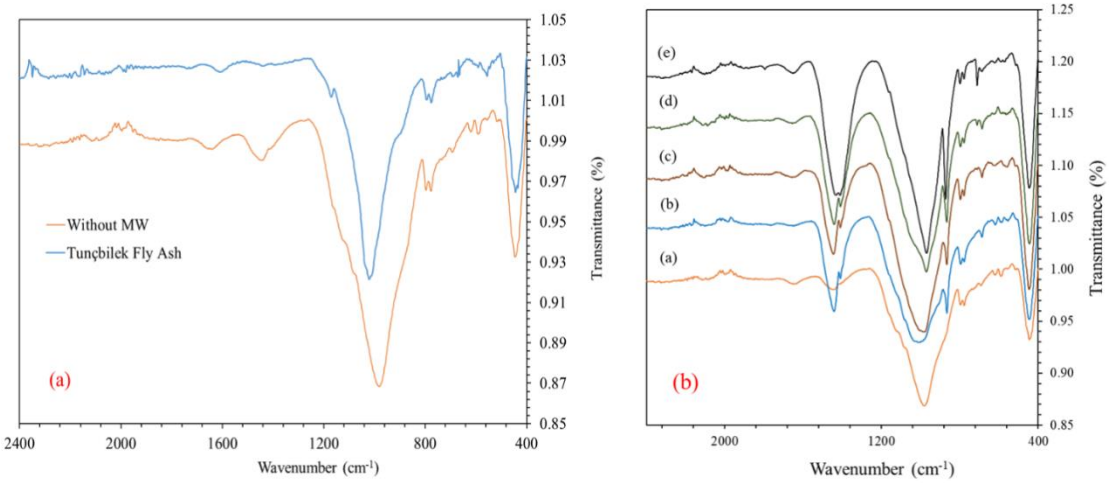

Figure 4. FTIR spectra of raw Tunçbilek FA and MW0 geopolymer (a) and geopolymers MW0 (a), MW5 (b), MW10 (c), MW20 (d), and MW40 (e) (b).

Figure 4b shows the FTIR spectra of alkali activated compositions MW0, MW5, MW10, MW20, and MW40. With the addition of the MW, new peaks at frequencies of 1409, 866, 712 cm^{-1} were detected. These peaks indicated the presence of calcite and their intensities increased with the increase in the MW addition. The FTIR peak at 983 cm^{-1} (MW0) indicating geopolymerization shifted towards lower wavenumbers 979 (MW5), 969 (MW10), 968 (MW20), and 965 cm^{-1}(MW40) with increasing MW ratios. This result herein could not be interpreted in a similar way to the above discussion for Figure4a because of the gradual replacement of FA by increasing MW ratio in geopolymer compositions. There were several articles on the formation and co-existence

of the C-S-H phase within the geopolymer binder in the presence of significant amounts of calcium. A previous study reported that geopolymers with a high amount of Ca generated C-A-S-H phase along with the geopolymeric gel of N-A-S-H. In geopolymerization, Si^{4+} or Al^{3+} species react with Ca^{2+}, either in the FA or from external calcium-containing additive, to form calcium silicate hydrate gel (C-S-H), calcium alumino hydrate gel (C-A-H) or calcium aluminosilicate hydrate gel (C-A-S-H) in the presence of water[40,45-48]. Therefore, in the present study, the presumption explained in the following lines was adopted. During geopolymerization reactions, CaO from the MW ($CaCO_3$) was attacked by the alkali activation solution and turned into active species of Ca^{2+} and O^{2-}. The resultant active Ca^{2+} ions, along with Si^{4+} and Al^{3+} from the dissolution of reactive glassy FA microspheres, reacted with OH^- ions of alkali solution. Thus, C-A-S-H and N-A-S-H geopolymer gel formed[48]. It is thought that increasing MW content introduced more Ca^{2+} ions into the solution and accelerated the continuous development of geopolymer matrix, while the formation of C-S-H and C-A-S-H phases was promoted, which reflected itself as shifts in FTIR peaks towards lower wavenumbers[41,49]. These structures were expected to contribute to new phases in the sintering process and provide advantages in preserving material integrity.

Table 3. Physical and mechanical properties of sintered porous geopolymers.

Sample code	Apparent porosity (%)	Water absorption (%)	Bulk density (g/cm^3)	Linear shrinkage (%)	Flexural strength (MPa)	Compressive strength (MPa)
MW0	12.70	8.92	1.42	-0.70	19.85	34.98
MW5	16.38	10.55	1.55	1.44	15.30	31.74
MW10	22.87	14.84	1.54	1.71	12.02	27.00
MW20	31.41	20.85	1.51	1.15	6.14	17.50
MW40	39.92	28.17	1.42	0.81	5.35	12.00

Table 3 shows the change in apparent porosity and water absorption with the addition of increased MW. CO_2 gas, released on the decomposition of calcite[30,31,50,51] in the MW (equation 2), exerted pressure against the glassy phase of appropriate viscosity formed during sintering, leading to pore formation. An increase in the MW content increased apparent porosity and water absorption because of increasedpore formation. While the apparent porosity and the water absorption of MW0 were respectively 12.7 and 8.92%, they increased to respective ratios of 39.92 and 28.17% in MW40. Thisresult translates itself to more than a three-fold increase in apparent porosity and water absorption values. An increase in apparent porosity and water absorption with increasing content of the MW followed similar trends (Table 3) because water absorption directly relates to the open porosity of the sintered ceramics. When compared with the apparent porosity values of porous ceramics, produced from FA and MW/or calcite wastes by various other methods for different application areas, 39.92% open porosity value of MW40 was satisfactory and even better than those of the previous studies[25]. The water absorption values were in line[41]with or even better than that of the literature[24]. Furthermore, the apparent porosity value of MW40 (39.92%) was also in good agreement with those of open-pore ceramics produced from different raw materials by various other methods[52,53]. However, it must be borne in mind that all those studies in the literature were carried out for much longer holding times, and most of them at much higher sintering temperatures.

In Table 3, the variation in bulk density and linear firing shrinkage with an increase in the MW ratio was depicted. The bulk density of the sintered alkali-activated specimens slightly decreased, as expected, with increasing apparent porosity (Table 3). MW0 composition of high melting point (1220°C) was successfully sintered at the low temperature of 900°C. High sintering temperatures between 1050-1300°C are needed to sinter F class FA[54-57]. Previous research reported that alkali activation was successful in the performance enhancement of ceramics sintered at the low temperatures[21,58]. The reason for lower temperature sintering of MW0 specimen at 900°C was the alkali activation of the Tunçbilek FA before sintering. The material produced from FA, not subjected to alkali activation, could not be sintered at 900°C, and therefore could not maintain its integrity. The bulk density increased from 1.42 to 1.55 g/cm^3 at 5 wt. % MW (MW5) and then slightly decreased

with increasing ratio of the MW down to 1.42 g/cm^3 at MW40 composition. The first increase at 5 wt. % MW ratio may be because of an increasing amount of glassy phase formed by the fluxing action of calcite, which filled the pores in the structure and resulted in densification. In other words, calcite acted as a flux rather than acting as a pore-forming agent at this composition[36]. As the apparent porosity increased with the addition of the MW, the expected decrease in bulk density was not observed[31,32,35,50,51]. It is thought that this was because the MW used as a pore-making agent contained a high proportion of CaO (specific gravity 3.34 gr/cm^3). Therefore, although the apparent porosity increased, there was no significant change in the bulk density value.

Linear firing shrinkage also increased from almost 0 to 1.44% at MW5 and 1.71% at MW10 compositions, due to improved sintering then slightly decreased similarly with further increase in the MW content down to 0.81% at MW40 composition. The decrease in linear firing shrinkage can be attributed to the expansion that occurred due to increasing MW content acting as a pore former during sintering.

Microstructural analyses of sintered porous geopolymers

Figure5 shows the SEM images of porous geopolymers produced with different amounts of the MW. The SEM micrograph of MW0 in Figure5a showed that the structure had open and closed pores with thick pore walls. The structure was dense due to intense sintering at MW0 composition with a low apparent porosity value of 12.7% (Table 3). Due to the breakdown of $CaCO_3$ structure during sintering and the resulting CO_2 gas, the porosity increased in microstructures (Figure5b-e) as the MW ratio increased. Although the number of large pores of MW40 appeared less in Figure 5-e than those of other compositions, it was, indeed, the specimen with the highest apparent porosity (39.92%) (Table 3). Therefore, MW0 and MW40 porous specimens were compared with each other at high magnification in Figure 6 to reveal this difference in porosity more clearly. It was observed that MW0 had large pores and its pore walls were dense (Figure 6a). On the other hand, the SEM analyses determined that MW40 contained many small pores. Consequently, the addition of the MW resulted in a more porous (39.92%) structure (Figure 6b).

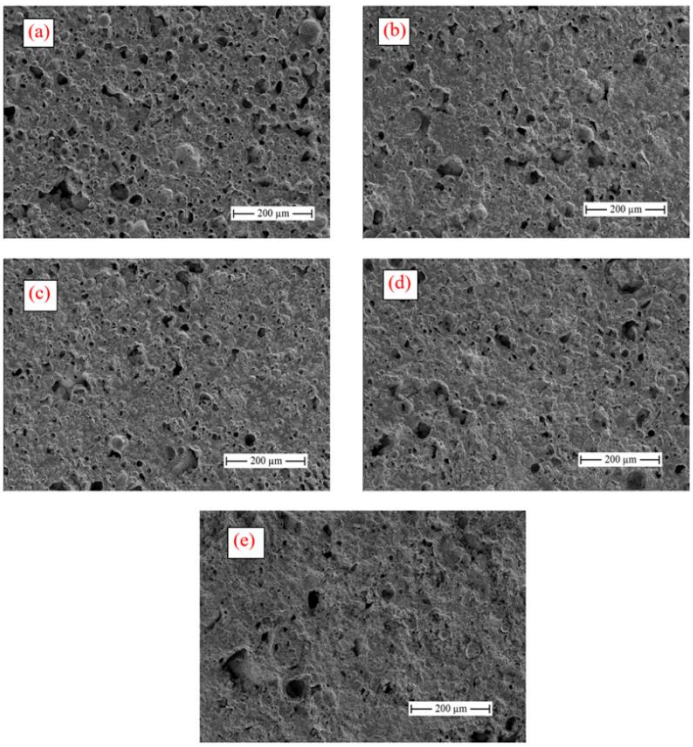

Figure 5. SEM analyses of sintered porous geopolymers MW0 (a), MW5 (b), MW10 (c), MW20 (d), MW40 (e).

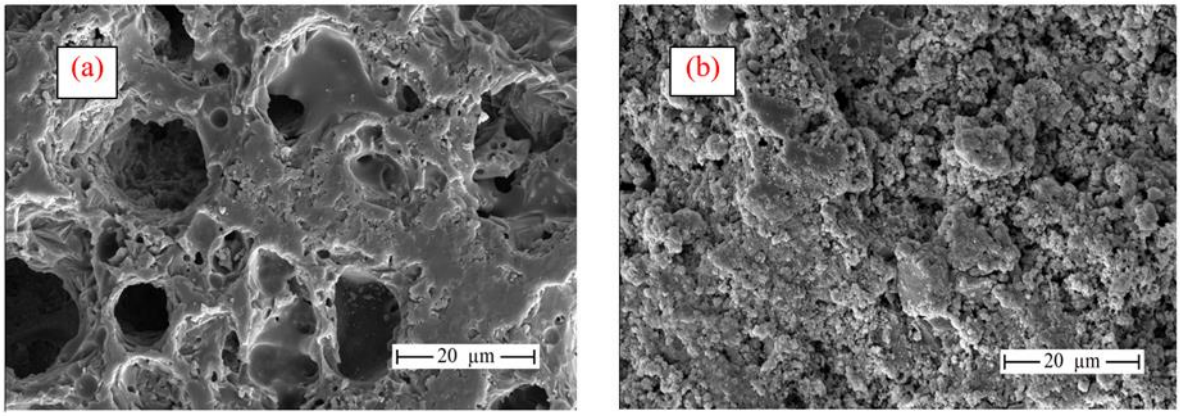

Figure 6.SEM analyses of sintered porous geopolymers; MW0 (a), MW40 (b).

Figure 7 shows the microstructure of the non-sintered MW40 composition. Compared with the microstructure after sintering (Figure 6b), the structure of the non-sintered specimen was dense, and the number of pores was low. However, after sintering, many new pores formed. Thus, a much more porous structure was observed by the removal of emitted CO_2 gas during the sintering process.

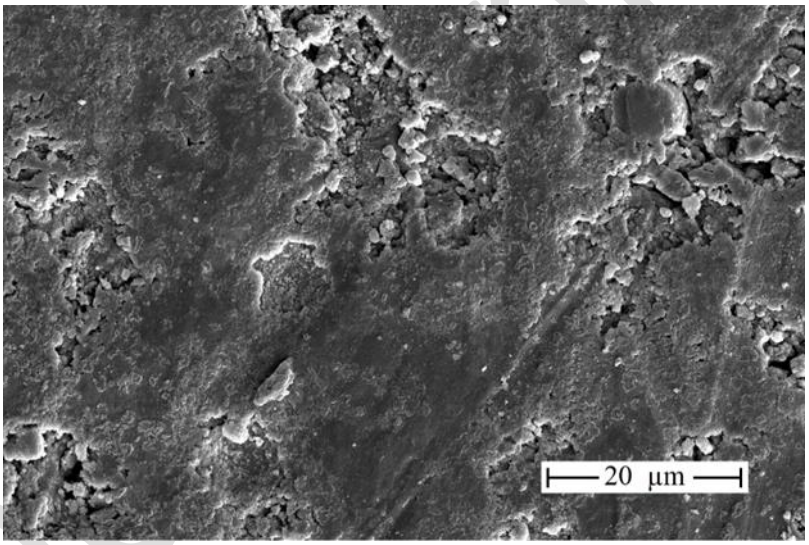

Figure 7. SEM image of non-sintered MW40 specimen

Phase evolution of sintered porous geopolymers

To study the crystalline phase evolution of fired alkali-activated specimens with increasing $CaCO_3$ (MW) addition was necessary for a better understanding of the modification of $CaCO_3$ on the pore structure. Figure 8 showed the XRD spectra and phase distribution of the specimens with different quantities of $CaCO_3$ sintered at 900 °C for 30 min. The Tunçbilek FA comprisedquartz, mullite, andhaematitewhilethe MW wascomposedmainly of calciteandquartz (Figure 1). However, the crystalline phases of quartz, mullite and haematite in the Tunçbilek FA and calcite in the MW disappeared and transformed into the new phases of gehlenite, nepheline, quartz, orthoclase and calcium iron oxide (Figure 8) upon sintering at 900°C. The main crystalline phases in the structure of sintered geopolymers were gehlenite and nepheline. The MW contained a very high earth alkali Ca (61,65 wt. % CaO) ratio and Mg (0.69 wt. % MgO). The SiO_2 content of the MW was 2.2 wt. %. On the other hand, the Tunçbilek FA contained earth alkali Ca (1.64 wt. % CaO), Mg (4,48 wt. % MgO) and the reasonably high content of Fe (11.45 wt. % Fe_2O_3). Besides, Na^+ ions were also present in the structure due to alkali activation. All these alkaline earth oxides along with Fe_2O_3have fluxing properties and it is thought that they contributed to the sintering of alkali-activated compositions at the low temperature of 900°C. This fluxing effect mayreflect itself as a lower glass phase viscosity, which helped to overcome the resistance

against the CO_2 pressure, leading to a porous structure. The phases of mullite, hematite, calcite in the fired geopolymers were totally, and quartz was partially consumed to develop new phases of gehlenite and nepheline (Table 2, Figure 1, Figure 8).

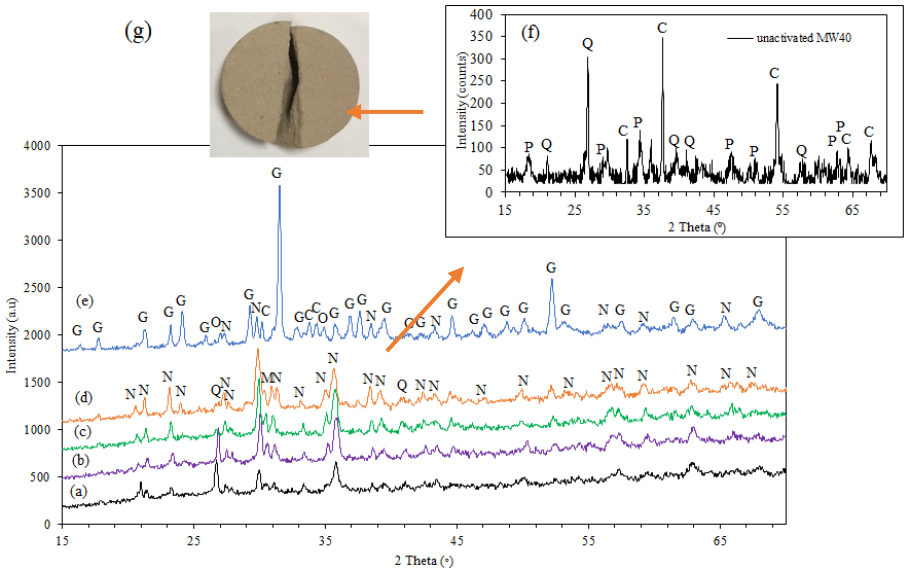

Figure 8. XRD spectra of sintered porous geopolymers; a) MW0, b) MW5, c) MW10, d) MW20, e) MW40, f) unactivated MW40, g) unactivated MW40 photograph (G: Gehlenite, N: Nepheline, Q: Quartz, O: Orthoclase, C: Calcium Iron Oxide, P: Portlantide ($Ca(OH)_2$))

Here, the addition of the MW had an effect on the phase structure formed. When the MW ratio was 5, 10 and 20 wt.%, the main phase was nepheline. However, when the MW addition was 40 wt.%, a low ratio of nepheline, orthoclase and calcium iron oxide phases developed in the structure, along with a large proportion of gehlenite phase. The absence of the free CaO phase was critical for the integrity and strength of the structure. The Na ions in the alkaline activation solution contributed toforming new phases such as nepheline and gehlenite at low temperature (900 °C), resulting in strong porousceramics. As seen in Figure 8f, a very different phase structure was obtained when the MW40 composition, which was not subjected to alkali activation, was sintered at 900°C. It was determined that there was free CaO at (a) high ratio,quartz, and $Ca(OH)_2$ formed from free CaO in this phase structure. The high amount of CaO is extremely unfavourable in terms of the integrity of the structure. As can be understood from here, it was shown in this study that using a material with high $CaCO_3$ content was possible with alkali activation. In addition, the sintered sample obtained when alkali activation was not applied was easily broken with a small force applied by hand (Figure 8g).Table 3 showed the variation in the compressive and flexural strength of the porous specimens obtained with increasing MW ratio. The addition of the MW caused a decline in mechanical properties. While this decline in strength was rapid up to 20 wt. % MW addition, it diminished at 40 wt. % MW addition. The porous specimen produced without the MW (MW0) had 34.98 MPa compressive and 19.85 MPa flexural strength values, while the 40 wt. % MW added porous specimen (MW40) had 12 MPa compressive and 5.35 MPa flexural strength values. The decrease in strength values was consistent with the increased apparent porosity. However, they were acceptable for open-pore materials[53].

CONCLUSION

The low-cost porous ceramics with sufficient apparent porosity and mechanical properties were successfully fabricated entirely from waste materials FA and MW. The experimental compositions were first alkali activated and then sintered at low temperature(900 °C). The MW with high $CaCO_3$ content was used for the first time as a pore-making agent at ratios between 5-40 wt. %. It was demonstrated that an increase in the MW amount had a

positive effect on the open porosity and the porosity increased proportionally with increasing MW amount. The maximum apparent porosity of the FA based open-pore ceramic containing 40 wt. % MW was 39.92%. The corresponding flexural and compressive strength values were found to be 5.35 and 12 MPa, respectively. The maximum amount of MW (40 wt. %) used in the present study was the highest in the related literature. Besides, alkali activation enabled the formation of main phases such as gehlenite (at 40 wt. % MW) and nepheline (at 0-20 wt. % MW) without free CaO in the structure as a result of the sintering process depending on the FA and MW ratios. This study showed that MW, which is an alternative waste material to $CaCO_3$ containing pore-making agents, could be used as a pore-making agent. The porous ceramic has the potential for use as a water purification membrane.

DECLARATIONS

Conflict of interest The authors declare that they have no conflict ofinterest.

REFERENCES

[1]. Das D, Kayal N. Thermal Shock Resistance of Porous Silicon Carbide Ceramics Prepared Using Clay and Alumina as Additives. Trans Indian Ceram Soc. 2019;78(3):165–171. https://doi.org/10.1080/0371750X.2019.1665478

[2]. Şan O, Koç M, Cengizler H. Production of porous ceramic from clinoptilolite incorporating aluminum powder. Ceram Int. 2019;45(18):24037–24043. https://doi.org/10.1016/j.ceramint.2019.08.108

[3]. Mustaffar MI, Mahmud MH. Processing of highly porous glass ceramic from glass and fly ash wastes. AIP Conf Proc. 2018;2031. https://doi.org/10.1063/1.5066966

[4]. Dong Y, Liu X, Ma Q, Meng G. Preparation of cordierite-based porous ceramic micro-filtration membranes using waste fly ash as the main raw materials. J Memb Sci. 2006;285(1–2):173–181. https://doi.org/10.1016/j.memsci.2006.08.032

[5]. Wehling J, Köser J, Lindner P, et al. Silver nanoparticle-doped zirconia capillaries for enhanced bacterial filtration. Mater Sci Eng C. 2015;48:179–187. https://doi.org/10.1016/j.msec.2014.12.001

[6]. Sun Z, Bai C, Zheng S, Yang X, Frost RL. A comparative study of different porous amorphous silica minerals supported TiO2 catalysts. Appl Catal A Gen. 2013;458:103–110. https://doi.org/10.1016/j.apcata.2013.03.035

[7]. Hu LF, Wang CA. Effect of sintering temperature on compressive strength of porous yttria-stabilized zirconia ceramics. Ceram Int. 2010;36(5):1697–1701. https://doi.org/10.1016/j.ceramint.2010.03.009

[8]. Bories C, Borredon ME, Vedrenne E, Vilarem G. Development of eco-friendly porous fired clay bricks using pore-forming agents: A review. J Environ Manage. 2014;143:186–196. https://doi.org/10.1016/j.jenvman.2014.05.006

[9]. Malik N, Bulasara VK, Basu S. Preparation of novel porous ceramic microfiltration membranes from fly ash, kaolin and dolomite mixtures. Ceram Int. 2020;46(5):6889–6898. https://doi.org/10.1016/j.ceramint.2019.11.184

[10]. Zong Y, Wan Q, Cang D. Preparation of anorthite-based porous ceramics using high-alumina fly ash microbeads and steel slag. Ceram Int. 2019;45(17):22445–22451. https://doi.org/10.1016/j.ceramint.2019.08.003

[11]. Galán-Arboledas RJ, Cotes T, Martínez C, Bueno S. Influence of waste addition on the porosity of clay-based ceramic membranes. Desalin Water Treat. 2016;57(6):2633–2639. https://doi.org/10.1080/19443994.2015.1017011E.

[12]. Al-Qadhi E, Li G, Ni Y. Influence of a Two-Stage Sintering Process on Characteristics of Porous Ceramics Produced with Sewage Sludge and Coal Ash as Low-Cost Raw Materials. Adv Mater Sci Eng. 2019;2019. https://doi.org/10.1155/2019/3710692

[13]. Cusidó JA, Cremades L V, Soriano C, Devant M. Applied Clay Science Incorporation of paper sludge in clay brick formulation : Ten years of industrial experience. Appl Clay Sci. 2015;108:191–198. https://doi.org/10.1016/j.clay.2015.02.027

[14]. Vlasova M, Rosales I, Kakazey M, Parra AP, Guardian R. Formation of Porous Ceramics Using Cullet and Biological Waste of Water Purification. Sci. Sinter.2011; 43:81-94 (January). https://doi.org/10.2298/SOS1101081V

[15]. Gislon ES, Simão L, Coelho K. Permeability of Porous Ceramic Membranes Obtained from Waste of

the Coal Extraction Process. 2016;(November). https://doi.org/10.4028/www.scientific.net/MSF.881.357

[16]. Ho C, Lo H, Lin K, Lan J. Characteristics of Porous Ceramics from Prepared from Sandblasting Waste and Waste Diatomite by Co-Sintering Process. 2018;00(00):1–8. https://doi.org/10.1002/ep.12942

[17]. Manni A, El A, Amrani I El, Hassani E, El A, Sadik C. Valorization of coffee waste with Moroccan clay to produce a porous red ceramics (class BIII). Boletín la Soc Española Cerámica y Vidr. 2019;58(5):211–220.https://doi.org/10.1016/j.bsecv.2019.03.001

[18]. Wang Q, Yu H, Ben T, et al. Preparation of lightweight high-strength thermal insulation and decoration integration porous ceramics using red mud. 2019.

[19]. Aziz IH, Mustafa M, Bakri A, et al. Manufacturing parameters influencing fire resistance of geopolymers : A review. 2016;0(0):1–13. https://doi.org/10.1177/1464420716668203

[20]. Rickard WDA, Temuujin J, Van Riessen A. Thermal analysis of geopolymer pastes synthesised from five fly ashes of variable composition. J Non Cryst Solids. 2012;358(15):1830–1839. https://doi.org/10.1016/j.jnoncrysol.2012.05.032

[21]. Jaya NA, Mustafa M, Bakri A, et al. Kaolin Geopolymer as Precursor to Ceramic Formation. 2016;01061.

[22]. Rickard WDA, Kealley CS, Riessen A Van. Thermally Induced Microstructural Changes in Fly Ash Geopolymers : 2015;939:929–940. https://doi.org/10.1111/jace.13370

[23]. Villaquirán-Caicedo MA, Gutiérrez RM De. Synthesis of ceramic materials from ecofriendly geopolymer precursors. 2018;230:300–304. https://doi.org/10.1016/j.matlet.2018.07.128

[24]. Al-Bakri Abdullah MM, Jamaludin L, Hussin K, Bnhussain M, Ghazali CMR, Ahmad MI. Fly ash porous material using geopolymerization process for high temperature exposure. Int J Mol Sci. 2012;13(4):4388–4395. https://doi.org/10.3390/ijms13044388

[25]. Sawan SEA, Zawrah MF, Khattab RM, Abdel-shafi AA. In-situ formation of geopolymer foams through addition of silica fume : Preparation and sinterability. Mater Chem Phys. 2020;239(June 2019):121998. https://doi.org/10.1016/j.matchemphys.2019.121998

[26]. ASTM C20-00, Standard Test Methods for Apparent Porosity, Water Absorption, Apparent Specific Gravity, and Bulk Density of Burned Refractory Brick and Shapes by Boiling Water, ASTM International, West Conshohocken, PA, 2015, www.astm.org

[27]. ASTM C67 / C67M-20, Standard Test Methods for Sampling and Testing Brick and Structural Clay Tile, ASTM International, West Conshohocken, PA, 2020, www.astm.org

[28]. ASTM C326-09, Standard Test Method for Drying and Firing Shrinkages of Ceramic Whiteware Clays, ASTM International, West Conshohocken, PA, 2018, www.astm.org

[29]. Standard Specification for Coal Fly Ash and Raw or Calcined Natural Pozzolan for Use in Concrete. 2018.M.

[30]. Sutcu M, Alptekin H, Erdogmus E, Er Y, Gencel O. Characteristics of fired clay bricks with waste marble powder addition as building materials. Constr Build Mater. 2015;82:1–8. https://doi.org/10.1016/j.conbuildmat.2015.02.055

[31]. Munir MJ, Abbas S, Nehdi ML, Kazmi SMS, Khitab A. Development of eco-friendly fired clay bricks incorporating recycled marble powder. J Mater Civ Eng. 2018;30(5):1–11. https://doi.org/10.1061/(ASCE)MT.1943-5533.0002259

[32]. Williams RP, Van Riessen A. Determination of the reactive component of fly ashes for geopolymer production using XRF and XRD. Fuel. 2010;89(12):3683–3692. https://doi.org/10.1016/j.fuel.2010.07.031

[33]. Hemmings RT, Berry EE. On The Glass In Coal Fly Ashes : Recent Advances. Mat. Res. Soc. Symp. Proc. Ontario Research Foundation, Sheridan Park, Mississauga, Ontario , 1988;113.

[34]. Hemmings RT., Berry EE., Cornelius BJ., Scheetz BE. in: McCarthy G.J., Glasser F.P., Roy D.M., Diamond S., Editors, Speciation in Size and Density Fractionated Fly Ash II. Characterization of a Low-Calcium, High-Iron Fly Ash., Mat. Res. Soc. Symp. Proc. Vol. 86, 1987, pp. 81–98. Norton,

[35]. Bilgin N, Yeprem HA, Arslan S, Bilgin A, Günay E, Maroglu M. Use of waste marble powder in brick industry. Constr Build Mater. 2012;29:449–457. https://doi.org/10.1016/j.conbuildmat.2011.10.011

[36]. Sokolář R, Vodová L, Grygarová S, Štubňa I, Šín P. Mechanical properties of ceramic bodies based on calcite waste. Ceram Int. 2012;38(8):6607–6612. https://doi.org/10.1016/j.ceramint.2012.05.046

[37]. Wons W, Rzepa K, Reben M, Murzyn P, Sitarz M, Olejniczak Z. Effect of thermal processing on the structural characteristics of fly ashes. J Mol Struct. 2018;1165:299–304. https://doi.org/10.1016/j.molstruc.2018.04.008

[38]. Terzi A, Pavlovi V. Novel Utilization of Fly Ash for High-Temperature Mortars : Phase Composition, Microstructure and Performances Correlation. Int J Appl Ceram Technol. 2015;146. https://doi.org/10.1111/ijac.12135

[39]. Dudric R, Cormos C, Imre F, Bizo L, Misca R. Fly ash from thermal power plant , raw material for glass-ceramic. Environ Eng Manag J. 2013;12(2):337-342. https://doi.org/10.30638/eemj.2013.041

[40]. Xiaolu GUO, Huisheng SHI, Maosong LIN, Wenjing D. Effects of Calcium Contents in Class C Fly Ash Geopolymer. Adv Mat Res. 2013;687:508–513. https://doi.org/10.4028/www.scientific.net/AMR.687.508

[41]. Bakri AMM Al, Kamarudin H, Bnhussain M, Nizar IK, Rafiza AR, Zarina Y. The Processıng , Characterızatıon , and Properties of Fly Ash Based Geopolymer Concrete. Rev.Adv.Mater. 2012;30:90–97.

[42]. Alehyen S, Achouri MEL, Taibi M. Characterization , microstructure and properties of fly ash-based geopolymer. JMES. 2017;8(5):1783–1796.

[43]. Khan M-I, Azizli K, Sufian S, Siyal AA, Man Z. Sodium Silicate Free Geopolymer As Coating Material : Adhesion To Steel. 1st International Electronic Conference on Materials. 2014;(May). https://doi.org/10.3390/ecm-1-b016

[44]. Kioupis D, Kavakakis C, Tsivilis S, Kakali G. Synthesis and Characterization of Porous Fly Ash-Based Geopolymers Using Si as Foaming Agent. Advances in Materials Science and Engineering. 2018;2018.

[45]. Yip CK, Deventer JSJVAN. Microanalysis of calcium silicate hydrate gel formed within a geopolymeric binder. J Mater Sci. 2003;8:3851–3860.

[46]. Dong M, Feng W, May F, Elchalakani M, Li GK, Karrech A. Development of a High Strength Geopolymer by Novel Solar Curing. Ceram Int. 2017;43(14):11233–11243. https://doi.org/10.1016/j.ceramint.2017.05.173

[47]. Yu X, Chen L, Komarneni S, Hui C. Fly ash-based geopolymer : clean production , properties and applications. J Clean Prod. 2016;125:253–267. https://doi.org/10.1016/j.jclepro.2016.03.019

[48]. Azimi EA, AbdullahMMB, Vizureanu P et al. Strength Development and Elemental Distribution of Dolomite/Fly Ash Geopolymer Composite under Elevated Temperature. Materials. 2020;13:1015. https://doi:10.3390/ma13041015

[49]. Zhao X, Liu C, Zuo L, Wang L, Zhu Q, Wang M. Investigation into the effect of calcium on the existence form of geopolymerized gel product of fly ash based geopolymers. Cem Concr Compos. 2019;103(July 2018):279–292. https://doi.org/10.1016/j.cemconcomp.2018.11.019

[50]. Harabi A, Boudaira B, Bouzerara F, et al. Porous ceramic supports for membranes prepared from kaolin (DD3) and calcite mixtures. Acta Phys Pol A. 2015;127(4):1164–1166. https://doi.org/10.12693/APhysPolA.127.1164

[51]. Klosek-Wawrzyn E, Malolepszy J, Murzyn P. Sintering behavior of kaolin with calcite. Procedia Eng. 2013;57:572–582. https://doi.org/10.1016/j.proeng.2013.04.073

[52]. Studart R, Gonzenbach UT, Tervoort E, Gauckler LJ. Processing Routes to Macroporous Ceramics: A Review. J Am Ceram Soc. 2006;89(6):1771–1789. https://doi.org/10.1111/j.1551-2916.2006.01044.x

[53]. Vakifahmetoglu C, Zeydanli D, Colombo P. Porous polymer derived ceramics. Mater Sci Eng R Reports. 2016;106:1–30. https://doi.org/10.1016/j.mser.2016.05.001

[54]. Biernacki JJ, Vazrala AK, Leimer HW. Sintering of a class F fly ash. Fuel. 2008;87:782–792. https://doi.org/10.1016/j.fuel.2007.08.024

[55]. Lingling X, Wei G, Tao W, Nanru Y. Study on fired bricks with replacing clay by fly ash in high volume ratio. Constr Build Mater. 2005;19:243–247. https://doi.org/10.1016/j.conbuildmat.2004.05.017

[56]. Biernacki JJ, Mogula NR, Dunne JK, Nagolu RR. Kinetics Of Sintering For A Class-F Fly Ash: A Sintering Model. Woodhead Publishing Limited; 2012 https://doi.org/10.1533/9780857099891.71

[57]. Erol M, Ku S. Characterization of sintered coal fly ashes. Fuel. 2008;87:1334–1340. https://doi.org/10.1016/j.fuel.2007.07.002

[58]. Luo Y, Ma S, Liu C, Zhao Z, Zheng S, Wang X. Journal of the European Ceramic Society Effect of particle size and alkali activation on coal fly ash and their role in sintered ceramic tiles. J Eur Ceram Soc. 2017;37(4):1847–1856. https://doi.org/10.1016/j.jeurceramsoc.2016.11.032